Am J Physiol Gastrointest Liver Physiol. Author manuscript; available in PMC 2017 January 17.

Published in final edited form as:

Am J Physiol Gastrointest Liver Physiol. 2004 August ; 287(2): G417–G424. doi:10.1152/ajpgi.00294.2003.

Expression of P2Y nucleotide receptors and ectonucleotidases in quiescent and activated rat hepatic stellate cells

Jonathan A. Dranoff[1], **Mika Ogawa**[2], **Emma A. Kruglov**[1], **Marianna D. A. Gaça**[3], **Jean Sévigny**[4], **Simon C. Robson**[2], and **Rebecca G. Wells**[3]

[1]Yale University School of Medicine and Yale Liver Center, New Haven, Connecticut 06520

[2]Harvard Medical School, Boston, Massachusetts 02215

[3]University of Pennsylvania School of Medicine, Philadelphia, Pennsylvania 19104

[4]Centre de récherche en Rhumatologie et Immunologie, Université Laval, Sainte-Foy, Quebec, Canada G1V 4G2

Abstract

Extracellular nucleotides regulate a variety of cellular activities, including proliferation of fibrogenic cells outside of the liver. However, the expression of receptors for extracellular nucleotides in hepatic stellate cells (HSC) is unknown. Thus our aims were to investigate the expression of mediators of nucleotide signaling in HSC and to determine whether extracellular nucleotides regulate HSC function. Confocal video microscopy was used to observe nucleotide-induced changes in cytosolic Ca^{2+}(Ca_i^{2+}) in live HSC. P2Y receptor subtype expression and ectonucleotidase expression in quiescent and activated HSC were determined using RT-PCR, Northern blot, immunoblot, and confocal immunofluorescence. Functional ectonucleotidase activity was assessed using a colorimetric method. Nucleotide-sensitive procollagen-1 mRNA expression in activated HSC was assessed using real-time RT-PCR. Extracellular ATP increased Ca_i^{2+} in HSC; this was inhibited by the P2 receptor inhibitor suramin. Quiescent HSC expressed the P2Y subtypes $P2Y_2$ and $P2Y_4$ and were activated by ATP and UTP, whereas activated HSC expressed the P2Y subtype $P2Y_6$ and were activated by UDP and ATP. Activated but not quiescent HSC expressed the ectonucleotidase nucleoside triphosphate diphosphohydrolase 2, extracellular UDP tripled procollagen-1 mRNA expression in activated HSC, and this was inhibited by the P2Y receptor inhibitor suramin. HSC express functional P2Y receptors and switch the expression of P2Y receptor subtypes on activation. Moreover, HSC differentially regulate nucleoside triphosphate diphosphohydrolase expression after activation. Because activation of P2Y receptors in activated HSC regulates procollagen-1 transcription, P2Y receptors may be an attractive target to prevent or treat liver fibrosis.

Keywords

P2Y receptor; nucleoside triphosphate diphosphohydrolase; ecto-nucleotidase; adenosine 5′-triphosphate receptor; fibrogenesis; cell proliferation

Address for reprint requests and other correspondence: J. A. Dranoff, Yale Univ. School of Medicine, Section of Digestive Diseases, 333 Cedar St. LMP 1080, New Haven, CT 06520 (jonathan.dranoff@yale.edu).

Hepatic Stellate Cells (HSC) are the primary fibrogenic cells of the liver. HSC in the normal liver are rich in vitamin A, with low levels of proliferation and extracellular matrix deposition and are termed “quiescent.” In the setting of chronic liver disease, or when cultured on plastic in vitro, they undergo a transdifferentiation into highly proliferative and fibrogenic myofibroblasts that are responsible for the bulk of abnormal matrix deposition in liver fibrosis and are termed “activated.” Although many of the signaling systems that regulate HSC activity have been elucidated in recent years (8, 13), a number of questions remains. Identification of novel signals regulating matrix deposition and HSC proliferation is of particular importance, because this may lead to novel prophylactic and therapeutic approaches to liver fibrosis.

Extracellular nucleotides act as signaling molecules through activation of specific receptors. Receptors for nucleotides are known as P2 receptors. These are further divided into ligand-gated P2X receptors and G protein-coupled P2Y receptors (28). P2 receptors have been shown to regulate a variety of cell functions, such as gene transcription (27), growth (3), apoptosis (29), secretion (23), contractility (24), and chemotaxis (22). Cloning of individual P2 receptor subtypes and detailed pharmacological experiments have begun to define the specific roles of these receptors in cell physiology. Ectonucleotidases have now been identified as critical regulators of P2 receptor activation. The ectonucleotidase nucleoside triphosphate diphosphohydrolase (NTPDase)-1 is a critical regulator of platelet activity (14). NTPDase2 is expressed in portal fibroblasts in normal rat liver, suggesting a role in regulation of bile ductular signaling (9). Thus there are both specific receptors for extracellular nucleotides and enzymatic regulators of those receptors.

Extracellular nucleotides are important regulators of proliferation and apoptosis in fibrotic mesangial cells of the kidney (20). Moreover, a prior report (32) has suggested that cultured HSC express functional nucleotide receptors. We hypothesized that both quiescent and activated HSC express specific P2Y receptors for extracellular nucleotides and ectonucleotidases and that these nucleotides are important regulators of activated HSC function. We report here that both quiescent and activated HSC express the necessary cellular machinery for nucleotide-mediated signaling, that HSC undergo a shift in expression of P2Y receptors and ectonucleotidases as they activate, and that activation of P2Y receptors in activated HSC regulates transcription of the matrix component α(1)-procollagen.

METHODS

Materials and reagents

ATP, apyrase, imidazole, ammonium molybdate, collagenase, Malachite green hydrochloride, suramin, alkaline phosphate-conjugated anti-rabbit secondary antibody, and mouse monoclonal anti-smooth muscle actin antibody were obtained from Sigma (St. Louis, MO). AlexaFluor 488 anti-rabbit antibody and AlexaFluor 594 were purchased from Molecular Probes (Eugene, OR). Pronase protease was obtained from Calbiochem (San Diego, CA) and Roche Molecular Biochemicals (Chicago, IL). M199 medium was purchased from Invitrogen (Carlsbad, CA). All other chemicals were of the highest quality commercially available.

Laboratory animals

Adult male Sprague-Dawley rats were used for all experiments. Treatment of animals was within the prescribed guidelines of the Yale, Harvard, and University of Pennsylvania Institutional Animal Care and Use Committees.

For CCl_4 treatment, rats (180–250 g) were provided drinking water containing 1% phenobarbital starting 2 wk before and during the entirety of CCl_4 treatment, to upregulate cytochrome *P*-450 enzyme levels (21). Rats were injected subcutaneously with CCl_4 (0.1 ml, CCl_4 diluted 1:6 in olive oil) three times per wk for 6–8 wk. For control experiments, rats were injected in identical fashion with olive oil alone (CCl_4-free vehicle). Livers were harvested and fixed for immunofluorescence as described in *Confocal immunofluorescence*.

Isolation of HSC

HSC were isolated from retired breeder rats (500–700 g) by in situ pronase/collagenase perfusion followed by density gradient centrifugation, as described previously (1). Primary cells were >95% pure. Cells were grown on standard tissue culture plastic dishes in M199 medium with 10% fetal calf serum and antibiotics. Primary cells were used at either 1 or 7 days after isolation or were passaged after 7 days and used at *passages 1–4*. HSC at *day 1* after isolation are phenotypically quiescent, whereas cells at *day 7* are phenotypically activated (1).

RT-PCR

RNA was isolated from HSC using chaotropic methods. HSC cDNA was produced using SuperScript First-Strand Synthesis System for RT-PCR (Invitrogen) on DNase-treated RNA. Specific oligonucleotide primers designs based on the cloned rat P2Y subtypes $P2Y_1$, $P2Y_2$, $P2Y_4$, and $P2Y_6$ (10) were used to amplify *days 1* and *7* HSC cDNA using the following thermal cycling parameters: 94°C × 5 min; 30 cycles [94°C × 30 s, 60°C × 1 min (63°C for P2Y4), 72°C × 1 min]; 72°C × 5 min. Control reactions were performed with RT-treated RNA that was not subjected to DNase treatment. Products were evaluated using agarose gel electrophoresis.

In separate experiments, specific oligonucleotide primers designs based on the published sequence of rat NTPDase1 (GenBank accession no. NM-022587), NTPDase2 (NM-172030), NTPDase3 (NM_178106), NTPDase5 (NM-007647), and NTPDase6 (NM-053498) were used to amplify *days 1*, *4*, and *7* HSC cDNA using the following thermal cycling parameters: 94°C × 5 min; 30 cycles of 94°C × 30 s, 62°C × 1 min, and 72°C × 1 min; and 72°C × 10 min.

Real-time RT-PCR

Alterations in expression of α(1)-procollagen (procollagen-1) mRNA in activated HSC were determined using real-time RT-PCR. HSC were treated with either vehicle alone (control), suramin (50 μM), UDP (100 μM), or UDP + suramin every 24 h (for a total of 2 treatments) in a 48-h period. Total RNA was isolated as described above and subjected to real-time PCR using the-ABI-PRISM 7700 (Applied Biosystems, Foster City, CA). Detection of procollagen-1 was accomplished by labeling with 6-carbofluo-rescein (6-FAM) normalized

to a VIC-labeled GAPDH probe. PCR was performed using the following cycling parameters: reverse transcription at 48°C × 30 min; activation of Ampli *Taq* polymerase (Applied Biosystems) at 95°C × 10 min; PCR cycling 40 cycles of 95°C × 15 s (denaturation) and 60°C × 1 min (annealing/extention). Experiments were performed in triplicate and expressed in micrograms of procollagen-1 mRNA per milligram of total RNA.

Western blot analysis

Alterations in expression of NTPDase2 were determined by Western blot analysis using a rabbit polyclonal antibody directed against NTPDase2/CD39L1 (9, 31). Protein was isolated from HSC at 1, 4, and 7 days after isolation after osmotic lysis. Equal amounts of protein for each group were separated by SDS-PAGE and transferred onto a PVDF membrane (Immobilon; Milli-pore, Bedford, MA). The membrane was blocked with nonfat milk (5% in PBS + 0.05% Tween), hybridized to the anti-NTPDase2 antibody and then anti-rabbit secondary antibody, and developed using enhanced chemiluminescence.

Confocal immunofluorescence

Changes in distribution of NTP-Dase2 after CCl_4 treatment were determined using confocal immunofluorescence. Tissue was fixed by perfusion with 2% (wt/vol) paraformaldehyde in 0.075 M sodium phosphate, pH 7.3, cryopreserved overnight in 30% (wt/vol) sucrose, and frozen in isopentane/liquid nitrogen. After 5 μm-thick sections were quenched with 50 mM NH_4Cl and 3% (vol/vol) goat serum in PBS, they were labeled with a 1:25 dilution of anti-NTPDase2 antibody and a 1:800 dilution of anti-smooth muscle actin antibody for 45 min at 37°C and then washed and incubated with AlexaFluor 488 conjugated anti-rabbit secondary antibody and AlexaFluor 598-conjugated anti-mouse secondary antibody. Negative controls were stained with AlexaFluor 488-conjugated anti-rabbit secondary antibody plus AlexaFluor 598-conjugated anti-mouse secondary antibody without primary antibodies. Specimen fixation plus all washes and incubations included pepstatin (2 μM), PMSF (0.2 mM), and benzamidine (0.5 mM) to inhibit proteolysis.

Specimens were examined using a Zeiss LSM 510 confocal imaging system equipped with both a krypton/argon and helium/neon laser at ×400 magnification. Double-labeled specimens were serially excited at 488 nm and observed at >515 nm to detect AlexaFluor 488 and then excited at 568 nm and observed at >585 nm to detect AlexaFluor 598 using only the Krypton/Argon laser.

Assay of ectonucleotidase activity

Functional ectonucleotidase activity was determined in live HSC by colorimetric detection of P_i (30). Rat HSC were isolated as described in *Isolation of HEC* and plated in equal amounts on 24-well plastic plates. Cells were washed with nucleotide- and P_i-free incubation medium (in mM: 150 NaCl, 1.5 $CaCl_2$, 50 Tris, and 50 imidazole, pH 7.4) two times before use. Enzyme activity was determined in incubation medium containing 0.3 mM nucleotide (ATP, ADP, or AMP). The reaction was incubated at 37°C for exactly 8 min, and reactions were terminated by the addition of 0.25 ml of Malachite green reagent (5). Malachite green color change in response to P_i was detected by measuring the absorbance at

620 nm using a multiplate spectrometer (PowerWare 340; Bio-Tek Instruments, Winooski, VT).

Confocal video microscopy

Confocal video microscopy was performed using HSC grown on glass coverslips. HSC were loaded with the Ca^{2+}-sensitive fluorophore fluo-4/AM (Molecular Probes) and mounted on a specially designed stage for use on a confocal microscope. Cells were perifused initially with HEPES buffer, then with buffer containing ATP, ADP, UTP, or UDP (100 μM). Changes in fluo-4 fluorescence were monitored using a Bio-Rad MRC 600 confocal imaging system. Fluo-4 fluorescence was excited using a Kr/Ar laser at 488 nm; emitted fluorescence >515 nm was collected. Changes in fluorescence over time were expressed as peak fluorescence divided by initial fluorescence. Separate experiments were performed in the presence of P2Y inhibitor suramin (50 μM) in the initial buffer and the ATP-containing buffer and in Ca^{2+}-free media.

Statistical analysis

Data are expressed as means ± SD where appropriate. Comparisons between individual groups were made with two-tailed *t*-tests.

RESULTS

HSC express functional P2Y receptors

Functional expression of P2Y receptors in activated, passaged HSC was determined using confocal video microscopy to image changes in cytosolic Ca^{2+}(Ca_i^{2+}) in response to extracellular nucleotides. P2Y receptors induce downstream effects via inositol trisphosphate (IP_3)-mediated Ca_i^{2+} increases (11). As seen in the representative micrograph in Fig. 1, perifusion of passaged HSC with ATP (100 μM) induced a rapid and sustained increase in Ca_i^{2+}. Both sustained and oscillatory increases in Ca_i^{2+} were noted in separate experiments (Fig. 1*B*). These separate patterns of Ca^{2+} signals may be due to the distribution of different IP_3 receptors in HSC, although this remains to be elucidated (6, 19).

These Ca_i^{2+} increases were due to activation of P2Y receptors, because they were inhibited by the P2Y receptor inhibitor suramin but were unaltered by removal of extracellular Ca^{2+} even when measured at time points up to 5 min, and thus they were not dependent on Ca^{2+} influx (Fig. 2). Taken together, these findings demonstrate that HSC express functional P2Y receptors coupled to Ca_i^{2+} signals. These findings also demonstrate that nucleotide-mediated Ca_i^{2+} signals in HSC are triggered by P2Y receptors and not P2X receptors, because they occur in the absence of extracellular Ca^{2+}.

P2Y-mediated Ca_i^{2+} signals in HSC are simultaneous and not polarized. Because downstream effects of hormone-mediated Ca_i^{2+} signals in epithelia result, in part, from special and temporal gradients in Ca_i^{2+} (25), we investigated whether there was evidence for Ca^{2+} gradients or waves in HSC in response to extracellular nucleotides. To do this, we

performed post hoc analysis of Ca_i^{2+} signals in regions within HSC activated by extracellular nucleotides as demonstrated in Fig. 1. Because HSC lack tight junctions and thus do not have apical and basolateral plasma membrane domains (15, 16), regions of interest were determined empirically. As seen in Fig. 3, ATP-induced changes in Ca_i^{2+} occurred simultaneously throughout the cell, suggesting that Ca_i^{2+} signals are not localized to the nucleus (12) or other specific regions of HSC.

HSC alter their expression of P2 receptor subtypes on activation. The expression of specific P2Y receptor subtypes by *days 1* (quiescent) and *7* (activated) HSC was determined using molecular and functional methods. Four P2Y subtypes have been cloned in rat: $P2Y_1$, $P2Y_2$, $P2Y_4$, and $P2Y_6$. In rats, the ligand specificity for each of these is as follows: $P2Y_1$ (ADP), $P2Y_2$ and $P2Y_4$ (ATP = UTP), and $P2Y_6$ (UDP) (28).

The molecular expression of P2Y receptor subtypes in *days 1* and *7* HSC was demonstrated using RT-PCR with oligonucleotide primers specific to the cloned rat $P2Y_1$, $P2Y_2$, $P2Y_4$, and $P2Y_6$ receptors (10). As seen in Fig. 4*A*, *day 1* HSC expressed the P2Y subtypes $P2Y_2$ and $P2Y_4$, whereas *day 7* HSC expressed the P2Y subtypes $P2Y_6$ (intense band) and $P2Y_1$ (faint band).

The functional expression of P2Y receptor subtypes in *days 1* and *7* HSC was determined using confocal video microscopy (Fig. 4*B*). HSC were grown on glass coverslips, loaded with fluo-4/AM, mounted in a special perifusion chamber, and stimulated with a variety of nucleotides. Changes in fluo-4 fluorescence were plotted over time. Consistent with their expression of the triphosphate-specific receptors $P2Y_2$ and $P2Y_4$, *day 1* HSC were activated by ATP and UTP but not ADP nor UDP. Consistent with their expression of the UDP-sensitive receptor $P2Y_6$, *day 7* HSC were activated by UDP. However, *day 7* HSC were not activated by the $P2Y_1$ agonist ADP, suggesting that they either do not express appreciable quantities of $P2Y_1$ protein or that these receptors are not tightly coupled to HSC Ca_i^{2+} signals. Interestingly, *day 7* HSC were activated by ATP, suggesting that they may express an ATP-sensitive P2Y receptor distinct from $P2Y_2$ or $P2Y_4$.

These data demonstrate that both quiescent and activated HSC express functional P2Y receptors and that they switch expression of these receptors on activation.

Expression of ectonucleotidases varies on activation of HSC. Because ectonucleotidases of the NTPDase class are critical regulators of P2Y receptors (14, 17, 18), we investigated expression of cloned NTPDases in quiescent and activated HSC.

Because antibodies for immunoblot that detect rat NTP-Dase1 are not available, molecular expression of the five cloned rat NTPDases in HSC was determined using RT-PCR. RT-PCR was performed using oligonucleotide primers designed to correspond to the published sequence of rat NTPDase1 (GenBank accession no. NM-022587), NTPDase2 (NM-172030), NTP-Dase3 (NM-178106), NTPDase5 (NM-007647), and NTP-Dase6 (NM-053498) with RNA from HSC at 1, 4, and 7 days after isolation. As seen in Fig. 5*A*, *days 1*, *4*, and *7* HSC express NTPDase1 and NTPDase2 mRNA. *Day 4* HSC also express NTPDase6 mRNA. This ectonucleotidase may be less likely to contribute to hydrolysis of extracellular

nucleotides by HSC, because it is primarily a Golgi-associated ectonucleotidase (7), although a fraction of this protein is localized to the plasma membrane.

Immunoblot analysis of relative NTPDase2 levels in quiescent and activated HSC was performed using polyclonal antibodies to mouse NTPDase2 in *days 1*, *4*, and *7* rat HSC (Fig. 5*B*). Whereas no NTPDase2 protein was detected in *day 1* HSC, *day 4* HSC had the greatest expression of NTPDase2, and NTPDase2 expression persisted in *day 7* HSC.

Functional expression of ectonucleotidases in HSC was determined using a functional assay for the detection of P_i from ATP or other nucleotides (Fig. 5*C*) (5, 9). Both *days 1* and *7* had ectonucleotidase activity and were roughly equal in hydrolysis of ATP and ADP, suggesting that NTPDase1 may be an important mediator of nucleotide hydrolysis by HSC. However, the upregulation in NTPDase activity may be due to upregulation of NTPDase2. No hydrolysis of AMP was observed, which is consistent with the fact that NTPDases do not hydrolyze AMP.

These data demonstrate that activated, but not quiescent, HSC express the ectonucleotidase NTPDase2. Both quiescent and activated HSC may express NTPDase1, although the lack of available antibodies for immunoblot limits this conclusion. Furthermore, activated HSC express approximately twice as much ectonucleotidase activity as quiescent HSC.

NTPDase2 colocalizes with activated HSC in CCl_4 cirrhosis. To determine whether induction of NTPDase2 was observed in experimental cirrhosis, rats were treated with CCl_4 for 6 wk. Confocal immunofluorescence was used to determine whether NTPDase2 colocalized with α-SMA-positive activated HSC. As seen in Fig. 6*A*, NTPDase2 was expressed along several bridging fibrous bands between central areas of the liver. As seen in Fig. 6*B*, α-SMA was expressed in the same region. Figure 6*C* demonstrates colocalization of NTPDase2 and α-SMA. Figure 6*D* demonstrates that no NTPDase2 nor α-SMA fluorescence was detected in liver sections from control animals treated only with olive oil (CCl_4 vehicle). These findings are representative of 10 experimental and 5 control animals and demonstrate that NTPDase2 colocalizes with activated HSC in CCl_4 cirrhosis.

Extracellular UDP regulates transcription of procollagen-1 transcription by HSC via P2Y receptors. The role of P2Y receptors in regulation of procollagen-1 mRNA expression in *day 7* HSC was assessed using real-time RT-PCR. Because *day 7* HSC express the P2Y receptor $P2Y_6$ and respond to extracellular UDP (Fig. 4), HSC were stimulated with either control vehicle, suramin alone, UDP alone, or UDP plus suramin (Fig. 7). UDP roughly tripled transcription of procollagen-1 after 24 h, and this effect was partially blocked by suramin, suggesting that the effect was mediated via P2Y receptor activation. Because suramin alone had no effect, it is likely that either HSC do not secrete large amounts of extracellular nucleotides or that they do not secrete enough endogenous extracellular nucleotides to overcome ectonucleotidase activity to act in an autocrine fashion.

DISCUSSION

HSC are important targets of liver disease therapy, because they are the chief fibrogenic cells of the liver. Although excellent work has been done elucidating signal transduction in these

cells over recent years (4, 8, 15), there is still no effective treatment for liver fibrosis. Thus it is critical to search for new signaling mechanisms that regulate HSC activity. We now demonstrate that HSC express functional P2Y purinoceptors that regulate Ca_i^{2+} signals in both quiescent and activated HSC. The patterns of Ca^{2+} signals observed in HSC include both sustained Ca^{2+} increases that are thought to be important in exocytosis and Ca^{2+} oscillations that may be important for cell volume autoregulation following exocytosis (25, 26). These findings are consistent with those of Takemura et al. (32), in which extracellular nucleotides were found to link to IP_3 accumulation, Ca_i^{2+} increases, and contractility of cultured HSC. We have now established that the activation of these same receptors regulate procollagen-1 transcription by HSC, suggesting that P2Y receptors are a potentially new target in the treatment of liver fibrosis.

Why might HSC be stimulated by extracellular nucleotides? Although P2Y receptors are distributed widely throughout the body, their role in mediating response to injury might be expected. Regulated release of nucleotides may occur through a variety of mechanisms, including channel-mediated release and exocytosis. However, nonregulated release of nucleotides occurs after cell lysis, as may occur in hepatitis. Thus released nucleotides could act as trophic factors for cells that produce scar matrix, although this remains hypothetical in the liver. Similar findings have been noted, however, in fibrogenic kidney mesangial cells (2).

The relative roles of the ectonucleotidases NTPDase1 and NTPDase2 in HSC have only been determined, in part, based on the findings of this study. It is clear that NTPDase2 (CD39L1) is expressed in HSC activated by prolonged culture and in experimental fibrosis but not expressed in quiescent HSC. However, this ectonucleotidase has much greater activity for triphosphate nucleotides than for diphosphate nucleotides. Because both quiescent and activated HSC express relatively equipotent ectonucleotidase activity, NTPDase1 may be the more important ectonucleotidase regulating net ectonucleotidase activity of HSC. However, it is possible that HSC may express newer NTPDases that have not been defined on a molecular basis. In any case, the likely physiological role of these proteins is to minimize P2Y activation to prevent receptor desensitization, as occurs in the NTPDase1 null mouse (14). The outcome of NTPDase1 and NTPDase2 blockade or knockout in liver fibrosis, however, remains to be addressed.

In summary, both quiescent and activated HSC express the necessary cellular machinery for nucleotide-mediated signaling: nucleotide-mediated Ca_i^{2+} signals, P2Y receptors, and ectonucleotidases that may regulate those receptors. Furthermore, extracellular UDP may regulate fibrogenesis by activated HSC via regulation of procollagen-1 transcription.

Acknowledgments

GRANTS

This work was supported by National Institute of Diabetes and Digestive and Kidney Diseases (NIDDK) Grant DK-02379 (to J. A. Dranoff), Pilot Project Grant DK-34989 from the Yale Liver Center (to J. A. Dranoff), research awards from the American Liver Foundation and The Canadian Institutes of Health Research (to J. Sévigny), NIDDK Grant DK-58123 (to R. G. Wells), and the University of Pennsylvania NIDDK Center for the Study of Digestive and Liver Diseases Grant P30-DK-50306.

References

1. Aguirre-Ghiso JA, Estrada Y, Liu D, Ossowski L. ERK(MAPK) activity as a determinant of tumor growth and dormancy; regulation by p38(SAPK). Cancer Res. 2003; 63:1684–1695. [PubMed: 12670923]
2. Alpini G, Glaser S, Alvaro D, Ueno Y, Marzioni M, Francis H, Baiocchi L, Stati T, Barbaro B, Phinizy JL, Mauldin J, Lesage G. Bile acid depletion and repletion regulate cholangiocyte growth and secretion by a phosphatidylinositol 3-kinase-dependent pathway in rats. Gastroenterology. 2002; 123:1226–1237. [PubMed: 12360484]
3. Amadio S, D'Ambrosi N, Cavaliere F, Murra B, Sancesario G, Bernardi G, Burnstock G, Volonte C. P2 receptor modulation and cytotoxic function in cultured CNS neurons. Neuropharmacology. 2002; 42:489–501. [PubMed: 11955520]
4. Bataller R, Brenner DA. Hepatic stellate cells as a target for the treatment of liver fibrosis. Semin Liver Dis. 2001; 21:437–451. [PubMed: 11586471]
5. Baykov AA, Evtushenko OA, Avaeva SM. A malachite green procedure for orthophosphate determination and its use in alkaline phosphatase-based enzyme immunoassay. Anal Biochem. 1988; 171:266–270. [PubMed: 3044186]
6. Bezprozvanny I, Watras J, Ehrlich BE. Bell-shaped calcium-response curves of Ins(1,4,5)P3- and calcium-gated channels from endoplasmic reticulum of cerebellum. Nature. 1991; 351:751–754. [PubMed: 1648178]
7. Braun N, Fengler S, Ebeling C, Servos J, Zimmermann H. Sequencing, functional expression and characterization of rat NTPDase6, a nucleoside diphosphatase and novel member of the ecto-nucleoside triphosphate diphosphohydrolase family. Biochem J. 2000; 351:639–647. [PubMed: 11042118]
8. Brenner DA, Waterboer T, Choi SK, Lindquist JN, Stefanovic B, Burchardt E, Yamauchi M, Gillan A, Rippe RA. New aspects of hepatic fibrosis. J Hepatol. 2000; 32:32–38.
9. Dranoff JA, Kruglov EA, Robson SC, Braun N, Zimmermann H, Sevigny J. The ecto-nucleoside triphosphate diphosphohydrolase NTP-Dase2/CD39L1 is expressed in a novel functional compartment within the liver. Hepatology. 2002; 36:1135–1144. [PubMed: 12395323]
10. Dranoff JA, Masyuk AI, Kruglov EA, LaRusso NF, Nathanson MH. Polarized expression and function of P2Y ATP receptors in rat bile duct epithelia. Am J Physiol Gastrointest Liver Physiol. 2001; 281:G1059–G1067. [PubMed: 11557527]
11. Dranoff JA, Nathanson MH. It's swell to have ATP in the liver. J Hepatol. 2000; 33:323–325. [PubMed: 10952251]
12. Echevarria W, Leite MF, Guerra MT, Zipfel WR, Nathanson MH. Regulation of calcium signals in the nucleus by a nucleoplasmic reticulum. Nat Cell Biol. 2003; 5:440–446. [PubMed: 12717445]
13. Eng FJ, Friedman SL. Fibrogenesis. I. New insights into hepatic stellate cell activation: the simple becomes complex. Am J Physiol Gastrointest Liver Physiol. 2000; 279:G7–G11. [PubMed: 10898741]
14. Enjyoji K, Sevigny J, Lin Y, Frenette PS, Christie PD, Esch JS 2nd, Imai M, Edelberg JM, Rayburn H, Lech M, Beeler DL, Csizmadia E, Wagner DD, Robson SC, Rosenberg RD. Targeted disruption of cd39/ATP diphosphohydrolase results in disordered hemostasis and thromboregulation. Nat Med. 1999; 5:1010–1017. [PubMed: 10470077]
15. Friedman SL. Hepatic stellate cells. Prog Liver Dis. 1996; 14:101–130. [PubMed: 9055576]
16. Friedman SL, Roll FJ. Isolation and culture of hepatic lipocytes, Kupffer cells, and sinusoidal endothelial cells by density gradient centrifugation with Stractan. Anal Biochem. 1987; 161:207–218. [PubMed: 3578783]
17. Goepfert C, Imai M, Brouard S, Csizmadia E, Kaczmarek E, Robson SC. CD39 modulates endothelial cell activation and apoptosis. Mol Med. 2000; 6:591–603. [PubMed: 10997340]
18. Goepfert C, Sundberg C, Sevigny J, Enjyoji K, Hoshi T, Csizmadia E, Robson S. Disordered cellular migration and angiogenesis in cd39-null mice. Circulation. 2001; 104:3109–3115. [PubMed: 11748109]
19. Hagar RE, Burgstahler AD, Nathanson MH, Ehrlich BE. Type III InsP3 receptor channel stays open in the presence of increased calcium. Nature. 1998; 396:81–84. [PubMed: 9817204]

20. Harada H, Chan CM, Loesch A, Unwin R, Burnstock G. Induction of proliferation and apoptotic cell death via P2Y and P2X receptors, respectively, in rat glomerular mesangial cells. Kidney Int. 2000; 57:949–958. [PubMed: 10720948]
21. Hashimoto M, Kothary PC, Raper SE. Phenobarbital in comparison with carbon tetrachloride and phenobarbital-induced cirrhosis in rat liver regeneration. J Surg Res. 1999; 81:164–169. [PubMed: 9927535]
22. Honda S, Sasaki Y, Ohsawa K, Imai Y, Nakamura Y, Inoue K, Kohsaka S. Extracellular ATP or ADP induce chemotaxis of cultured microglia through Gi/o-coupled P2Y receptors. J Neurosci. 2001; 21:1975–1982. [PubMed: 11245682]
23. Hwang TH, Schwiebert EM, Guggino WB. Apical and basolateral ATP stimulates tracheal epithelial chloride secretion via multiple purinergic receptors. Am J Physiol Cell Physiol. 1996; 270:C1611–C1623.
24. Kitamura T, Brauneis U, Gatmaitan Z, Arias IM. Extracellular ATP, intracellular calcium and canalicular contraction in rat hepatocyte doublets. Hepatology. 1991; 14:640–647. [PubMed: 1916664]
25. Nathanson MH. Cellular and subcellular calcium signaling in gastrointestinal epithelium. Gastroenterology. 1994; 106:1349–1364. [PubMed: 8174894]
26. Nathanson MH, Burgstahler AD, Mennone A, Boyer JL. Characterization of cytosolic Ca^{2+} signaling in rat bile duct epithelia. Am J Physiol Gastrointest Liver Physiol. 1996; 271:G86–G96.
27. Pines A, Romanello M, Cesaratto L, Damante G, Moro L, D'Andrea P, Tell G. Extracellular ATP stimulates the early growth response protein 1 (Egr-1) via a protein kinase C-dependent pathway in the human osteoblastic HOBIT cell line. Biochem J. 2003; 373:815–824. [PubMed: 12729460]
28. Ralevic V, Burnstock G. Receptors for purines and pyrimidines. Pharmacol Rev. 1998; 50:413–492. [PubMed: 9755289]
29. Sellers LA, Simon J, Lundahl TS, Cousens DJ, Humphrey PP, Barnard EA. Adenosine nucleotides acting at the human P2Y1 receptor stimulate mitogen-activated protein kinases and induce apoptosis. J Biol Chem. 2001; 276:16379–16390. [PubMed: 11278310]
30. Sevigny J, Robson SC, Waelkens E, Csizmadia E, Smith RN, Lemmens R. Identification and characterization of a novel hepatic canalicular ATP diphosphohydrolase. J Biol Chem. 2000; 275:5640–5647. [PubMed: 10681547]
31. Sevigny J, Sundberg C, Braun N, Guckelberger O, Csizmadia E, Qawi I, Imai M, Zimmermann H, Robson SC. Differential catalytic properties and vascular topography of murine nucleoside triphosphate diphosphohydrolase 1 (NTPDase1) and NTPDase2 have implications for thromboregulation. Blood. 2002; 99:2801–2809. [PubMed: 11929769]
32. Takemura S, Kawada N, Hirohashi K, Kinoshita H, Inoue M. Nucleotide receptors in hepatic stellate cells of the rat. FEBS Lett. 1994; 354:53–56. [PubMed: 7957901]

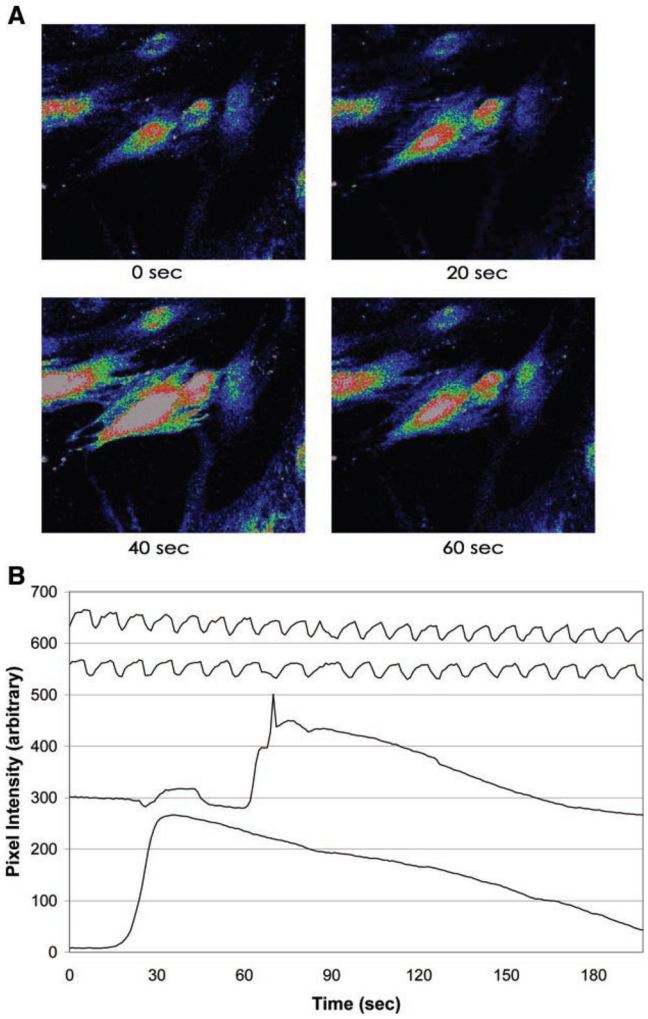

Fig. 1.

Extracellular ATP induces cytosolic Ca^{2+}(Ca_i^{2+}) signals in hepatic stellate cells (HSC). *A*: confocal micrographs of HSC perifused with ATP (100 μM) over time. HSC were loaded with the Ca^{2+}-sensitive dye fluo-4/AM and observed at 0.6-s intervals using a confocal microscope. HSC were peri-fused with HEPES buffer containing ATP (100 μM). An increase in fluo-4 fluorescence is seen first at 20 s and markedly at 40 s after addition of ATP in several HSC. *B*: graphic representation of Ca_i^{2+} signal in several individual HSC over time. Two patterns of Ca_i^{2+} signals are observed from separate HSC: sustained Ca^{2+} increases (seen in the *bottom* 2 tracings) and Ca^{2+} oscillations (*top* 2 tracings). Oscillations were less frequently seen than sustained Ca^{2+} increases (seen in 4 of 28 experiments). Changes in fluo-4 fluorescence were monitored using the narrowest possible pinhole settings, ensuring that changes in cell morphology would not affect fluorescence changes significantly. Note that the pixel intensities were shifted to avoid overlap of tracings.

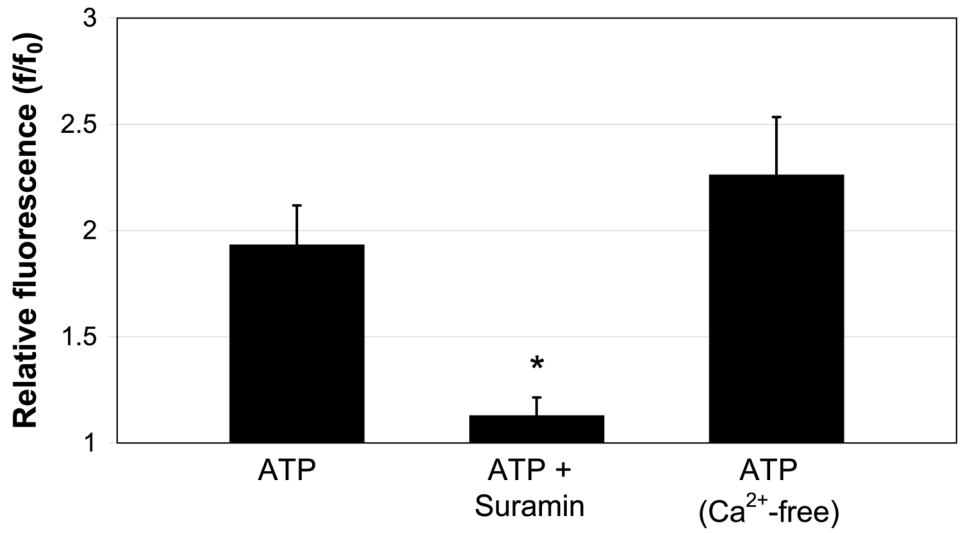

Fig. 2.

ATP-induced Ca_i^{2+} signals in HSC are due to activation of P2Y receptors. ATP-induced Ca_i^{2+} increases in HSC were investigated in the presence of the P2Y inhibitor suramin and in the absence of extracellular Ca^{2+}. Because the P2 receptor antagonist suramin inhibited ATP-induced Ca^{2+} increases, these increases were likely due to P2Y activation. Because removal of extracellular Ca^{2+} had no effect on ATP-induced Ca_i^{2+} increases, this suggests that these increases are due to mobilization of intracellular stores after activation of P2Y receptors rather than due to influx of extracellular Ca^{2+} after activation of P2X receptors. (*$P < 0.05$ vs. ATP)

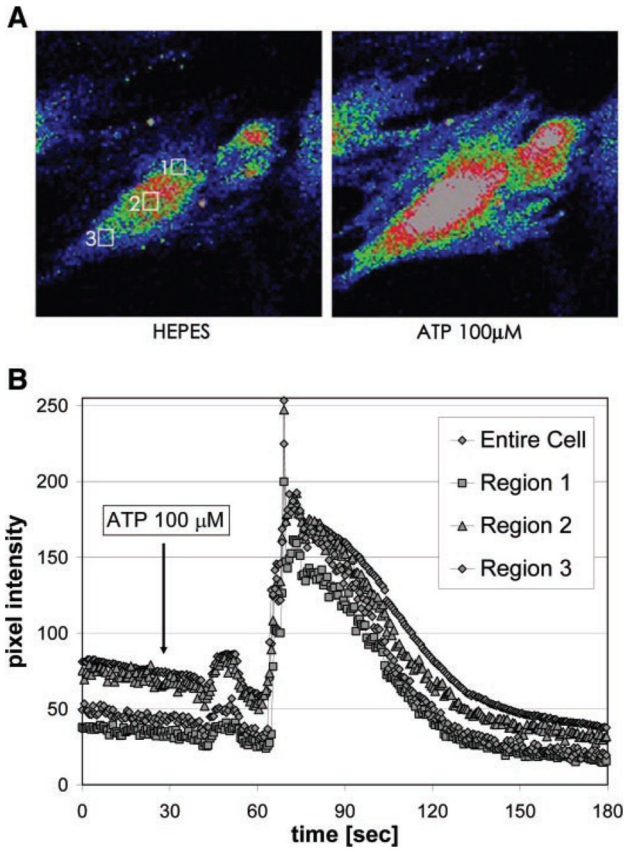

Fig. 3.

ATP-induced Ca_i^{2+} signals occur uniformly across HSC. *A*: microscopic display of regions of interest within an individual cell. A blow-up of the central cell seen in Fig. 1 is shown. Regions of interest were drawn on 3 different areas within the cell. *B*: graphical representation of Ca_i^{2+} signals within regions of interest depicted in *A*. fluo-4 fluorescence increases were plotted for the entire cell and for the 3 regions of interest identified in *A*. Unlike in some cell types, the fluorescence increases occur uniformly across the cell.

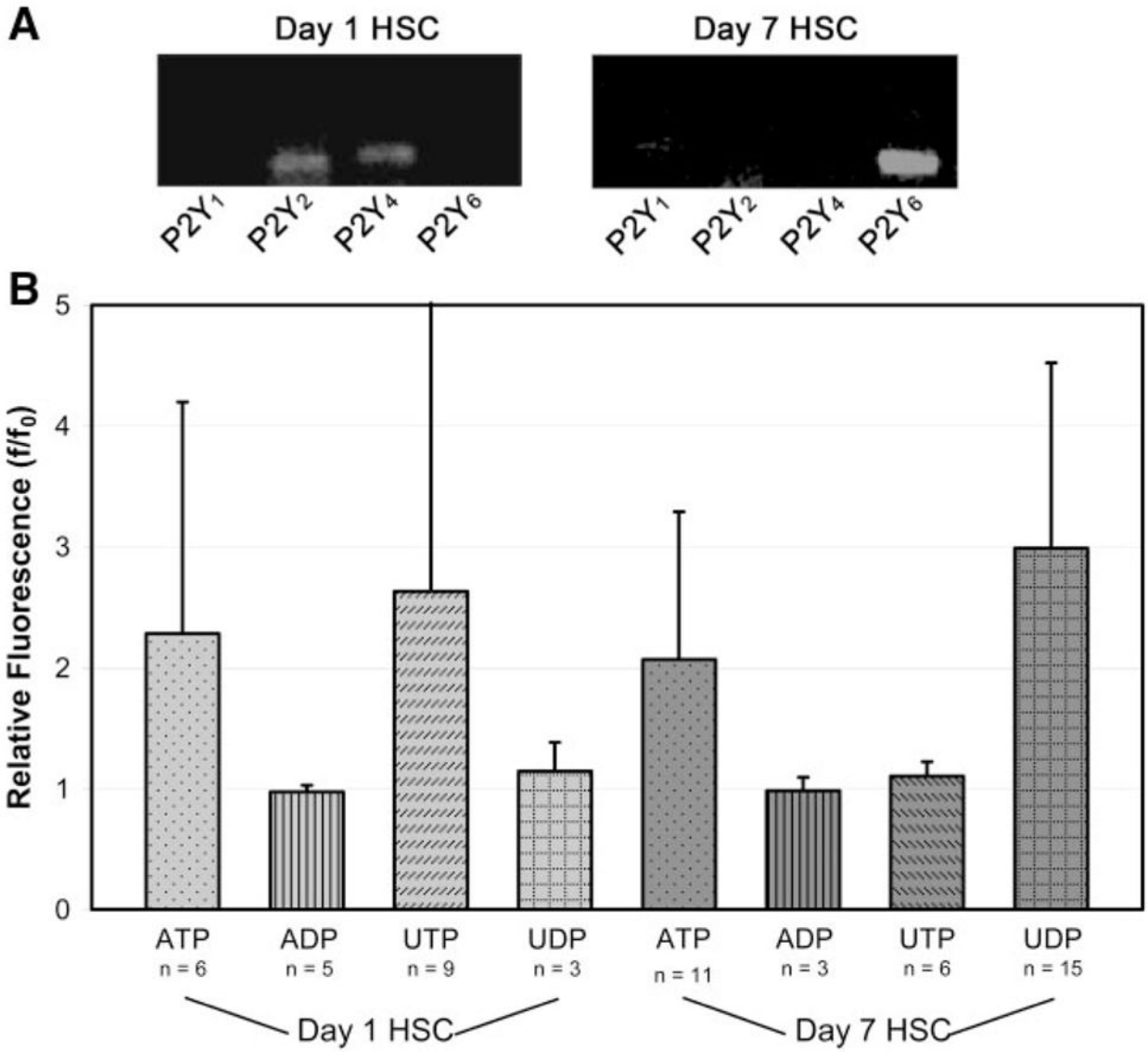

Fig. 4.

Quiescent HSC express the P2Y receptor subtypes $P2Y_2$ and $P2Y_4$, whereas activated HSC express the P2Y receptor subtype and $P2Y_6$. *A*: RT-PCR. RNA was isolated from HSC at 1 and 7 days after isolation and used for RT-PCR with oligonucleotides corresponding to the published sequences of the rat $P2Y_1$, $P2Y_2$, $P2Y_4$, and $P2Y_6$ (10). *Day 1* HSC express the ATP and UTP receptors $P2Y_2$ and $P2Y_4$, whereas *day 7* HSC express the UDP receptor $P2Y_6$. No bands were seen in RT negative controls (not shown). *B*: confocal video microscopy. Changes in fluo-4 fluorescence in HSC over time were calculated for the nucleotides ATP, ADP, UTP, and UDP in *days 1* and *7* HSC. Data are expressed as maximal fluorescence (f) divided by initial fluorescence (f_0). In *day 1* HSC, ATP and UTP induced a 2-fold increase in fluo-4 fluorescence. In *day 7* HSC, UDP induced a 3-fold increase in fluo-4 fluorescence, and ATP induced a 2-fold increase in fluo-4 fluorescence.

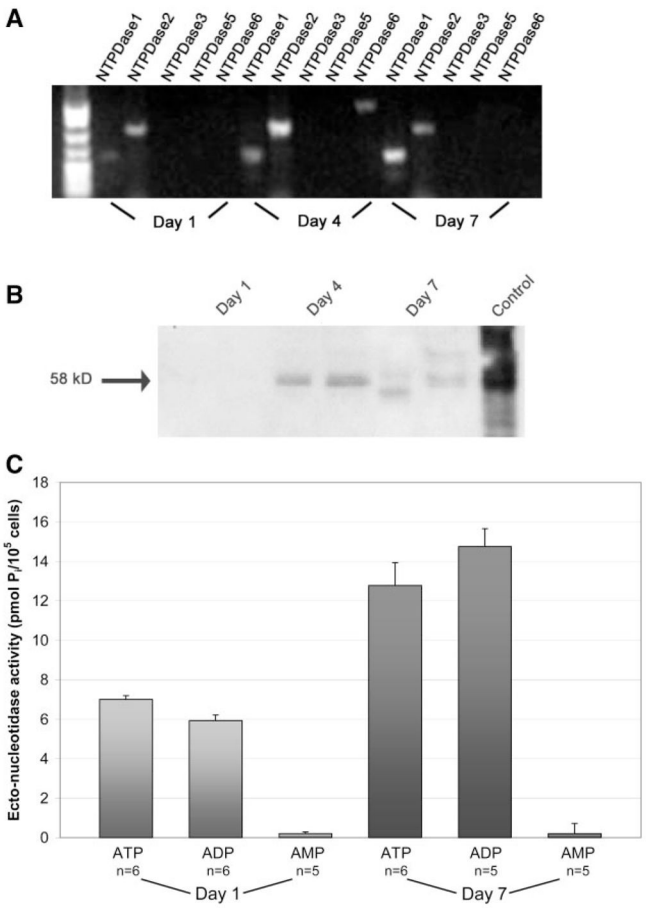

Fig. 5.

Nucleoside triphosphate diphosphohydrolase (NTPDase)2, but not NTPDase1, is upregulated in activated HSC. *A*: RT-PCR. RNA was isolated from *days 1*, *4*, and *7* HSC and used for RT-PCR, with oligonucleotides corresponding to the published sequence of the 5 cloned rat ecto-NTPDases (NTPDase1, NTPDase2, NTPDase3, NTPDase5, and NTPDase6; GenBank). HSC express mRNA for both NTPDase1 and NTPDase2. Only *day 4* HSC express the Golgi-associated UDPase NTPDase6 (7). *B*: immunoblot for expression of NTPDase2. Total protein fractions were isolated from *day 1* (quiescent), *day 4* (intermediate), and *day 7* (activated) HSC and subjected to PAGE, then immunoblotted with a polyclonal antibody to the mouse NTPDase2 (9). Bands are absent from *day 1* HSC but are strongest at *day 4* and remain present at *day 7*. Spleen protein was used as a positive control. Bands from the same column represent separate experiments. *C*: ectonucleotidase assay. Changes in ectonucleotidase function between *days 1* and *7* HSC were tested using the method of Baykov et al. (5). Because ectonucleotidase function is equal between ATP and ADP, NTPDase1 is likely an important mediator of ectonucleotidase function in HSC. Upregulation in nucleotide hydrolysis, however, may be mediated by the observed upregulation in NTPDase2.

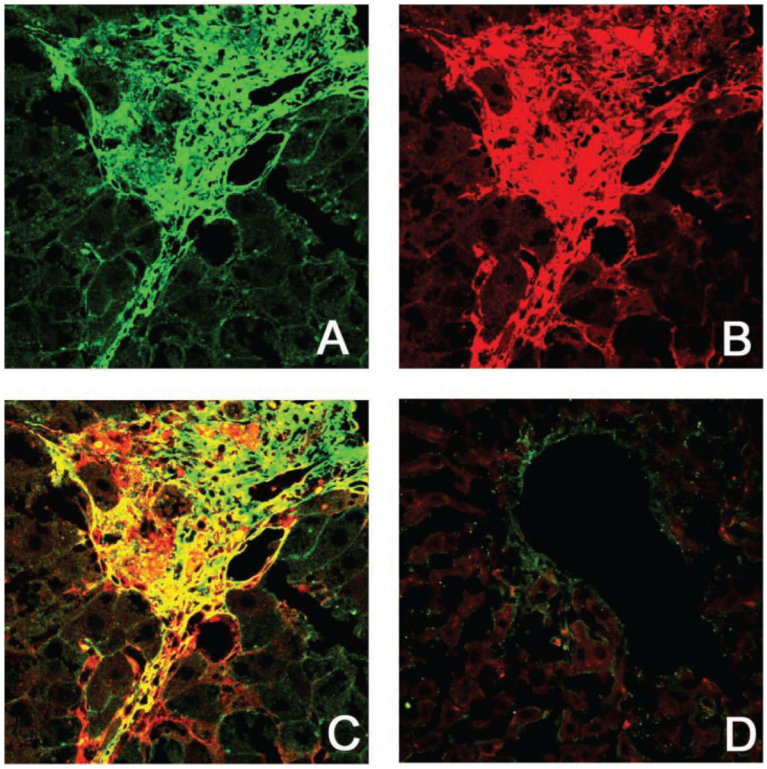

Fig. 6.

NTPDase2 is colocalized with α-smooth muscle actin (SMA) in fibrous bands bridging from central areas in CCl_4-induced cirrhosis. To determine whether NTPDase2 was localized with activated HSC in liver injury, rats were treated with CCl_4 for 6 wk. Confocal immunofluorescence was used to determine the expression of NTPDase2 and α-SMA. *A*: NTPDase2. NTPDase2 fluorescence is seen in green in a region of bridging fluorescence with several collapsed vessels. *B*: SMA fluorescence is seen in red in the same region. *C*: colocalization. Simultaneous red/green fluorescence demonstrates that NTPDase2 and SMA are expressed in the same region. *D*: negative control. Rats treated with olive oil alone (CCl_4 vehicle) show no NTP-Dase2 or SMA fluorescence.

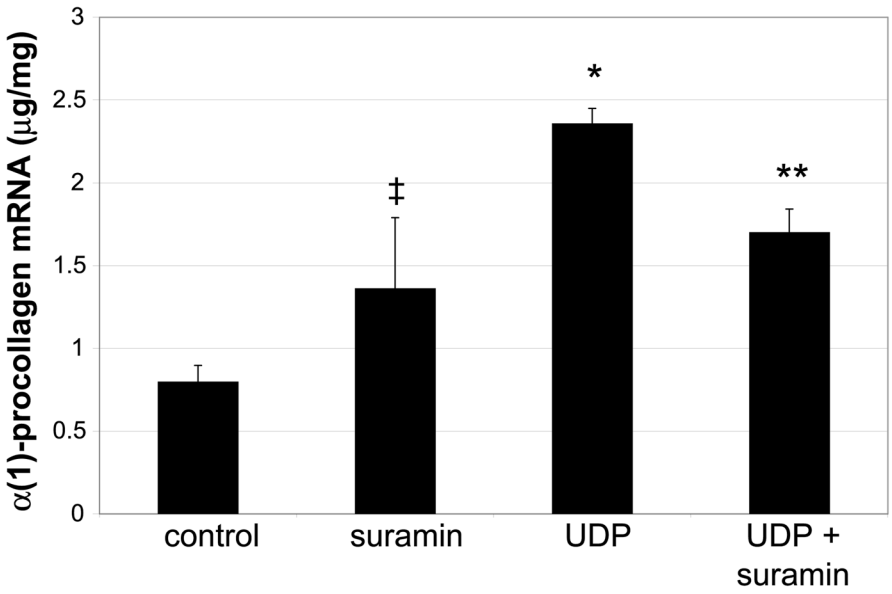

Fig. 7.

Extracellular UDP regulates transcription of a(1)-procollagen in activated HSC via P2Y receptor activation. Real-time RT-PCR was used to determine procollagen-1 mRNA content in *day 7* HSC treated under the following conditions: control (vehicle alone), suramin (50 mM), UDP (100 mM), or UDP + suramin. Suramin had no significant effect on procollagen-1 mRNA content. However, addition of UDP roughly tripled procollagen-1 mRNA, and this was partially inhibited by suramin addition (*$P < 0.01$ vs. control; **$P < 0.05$ vs. UDP, $P < 0.05$ vs. control; ‡P = not significant vs. control; $n = 3$ for all groups).